Majorana Fermions Under Uniaxial Stress in Semiconductor-Superconductor Heterostructures

Ming Gong[1,2], Li Mao[1,2], Sumanta Tewari[3], and Chuanwei Zhang[1,2*]
[1] *Department of Physics, the University of Texas at Dallas, Richardson, TX, 75080 USA*
[2] *Department of Physics and Astronomy, Washington State University, Pullman, WA, 99164 USA*
[3] *Department of Physics and Astronomy, Clemson University, Clemson, SC, 29634 USA*

Spin-orbit coupled semiconductor nanowires with Zeeman splitting in proximity contact with bulk s-wave superconductivity have recently been proposed as a promising platform for realizing Majorana fermions. However, in this setup the chemical potential of the nanowire is generally pinned by the Fermi surface of the superconductor. This makes the tuning of the chemical potential by external electrical gates, a crucial requirement for unambiguous detection of Majorana fermions, very challenging in experiments. Here we show that tunable topological superconducting regime supporting Majorana fermions can be realized in semiconductor nanowires using uniaxial stress. For n-type nanowires the uniaxial stress tunes the effective chemical potential, while for p-type systems the effective pairing may also be modified by stress, thus significantly enhancing the topological minigap. We show that the required stress, of the order of 0.1%, is within current experimental reach using conventional piezo crystals.

PACS numbers: 71.10.Pm, 03.67.Lx, 74.45.+c, 74.78.-w

Majorana fermions (MFs) are quantum particles which are their own antiparticles[1–3]. MFs are not only of fundamental interest because of their non-Abelian exchange statistics, but also may serve as building blocks for fault-tolerant topological quantum computation[4,5]. In the past few years, the possibility of realizing MFs using quasiparticles in exotic solid state systems[6–10] has generated a lot of excitement in the condensed matter community. In particular, it has been proposed recently that MFs can be generated using a heterostructure consisting of two very conventional materials: an s-wave superconductor and a semiconductor thin film/nanowire with strong spin-orbit coupling[11–20]. This proposal, following on the earlier idea proposed in cold atoms systems[21], has attracted widespread theoretical interest as well as serious consideration in experiments. Very recently, following the theoretical proposals, some preliminary experimental signatures[22–27] which may be related to the existence of MFs have been observed, although the unambiguous detection of MFs still remains an outstanding experimental challenge.

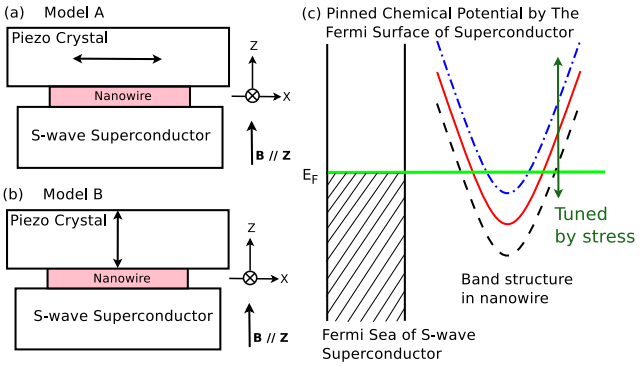

FIG. 1: (Color online). Engineering Majorana fermions via uniaxial stress. The stretching direction is along x in model A (a) and z in model B (b). The stress is assumed to be provided by conventional piezo crystals. (c) shows the pinning of the chemical potential in semiconductor by the Fermi surface of the s-wave superconductor. However, the total band structure of the semiconductor can still be shifted by uniaxial stress.

In the proposed semiconductor heterostructures, MFs only exist for topological superconducting states within a certain constrained parameter regime[13]. Therefore, it is crucially important to have the ability to tune various physical parameters in experiments. Since the spin-orbit coupling strength and the size of the nanowire cannot be tuned after the samples are fabricated, and the Zeeman field V_z is generally limited to a narrow window ($|V_z| \sim \Delta$, Δ is the superconducting pairing) because of its possible depairing effect, it is essential to be able to tune the chemical potential to the correct level for the realization of the topological state. For semiconductor nanowires, the chemical potential can be tuned by using suitably placed external electrical gates. Unfortunately, the same technique may not work well in the proposed Majorana system because the nanowire is in proximity contact with the superconductor which has an extremely high carrier density. The pinning of the chemical potential of the nanowire by the Fermi surface of the superconductor thus poses a major challenge in experiments[28]. In the recent Delft experiments[24] it has been found that very large electric gate voltages ($\sim (10^4 - 10^5)\Delta$) are required to tune the topological quantum phase transition, which likely provides strong evidence for the pinning of the nanowire chemical potential. The main motivation of the present work is to provide an alternative method to overcome this experimental difficulty which may greatly facilitate future experimental searches of MFs in semiconductor-based heterostructures.

In this Rapid Communication we show that the topological superconducting regime in both n- and p-type nanowires can be externally tuned using uniaxial stress,

which can be generated and controlled even by conventional piezo crystals. The uniaxial stress can modify the band structure of the nanowires slightly after the heterostructure system is fabricated, remarkably leading to a topological transition from the trivial to the topological superconducting state with MFs at the wire-ends. With the experimentally accessible strength of the uniaxial stress, the effective chemical potential can be tuned about 42 meV for electrons, and 5 - 20 meV for hole levels. Moreover, for the p-type systems, the uniaxial stress may also significantly enhance the minimum topological energy gap (minigap) that protects the MFs from thermal excitations. The newly added elements for generating the uniaxial stress can be effectively integrated into the design of semiconductor devices using modern nanotechnology. Therefore, our proposed scheme can go a long way in facilitating the realization and detection of Majorana fermions in semiconductor quantum wire heterostructures and the eventual implementation of topological quantum computation.

Our basic setup for experiments is illustrated in Fig. 1a and 1b. The semiconductor nanowire (e.g., InSb, InAs, etc.) is in proximity contact with an s-wave superconductor. The uniaxial stress applied on the semiconductor nanowires can be generated using nano-ferroelectric materials or by simply gluing the nanowire tightly to the surface of piezoelectric crystals[29–33] such as the piezoelectric lead zirconic titanate (PZT) ceramic stack. The stretching direction of the piezo crystal can be chosen either along x (model A) or along z direction (model B). The strain tensor can be determined as,

$$\varepsilon_{xx}^{(a)} = -\varepsilon, \quad \varepsilon_{yy}^{(a)} = \varepsilon_{zz}^{(a)} = \frac{2C_{12}}{C_{11}}\varepsilon,$$
$$\varepsilon_{zz}^{(b)} = -\varepsilon, \quad \varepsilon_{yy}^{(b)} = \varepsilon_{xx}^{(b)} = \frac{2C_{12}}{C_{11}}\varepsilon, \qquad (1)$$

where $\varepsilon = (1 - a/a_0)$ defines the relative changes of the lattice constant along the corresponding crystallographic directions. Here a_0 and a are the equilibrium and distorted lattice constants, respectively. $\varepsilon > 0 (< 0)$ corresponds to compressive (tensile) stress. In experiments the sign of ε can be controlled by the voltage bias across the piezo crystals[29–33]. C_{11} and C_{12} are the elastic stiffness tensors. The superscripts in Eq. (1) represent the two different models shown in Fig. 1. Note that $\varepsilon \sim \mathcal{P}/\mathcal{Y}$, where $\mathcal{P}$ is the stress and $\mathcal{Y}$ is Young's modulus. Using typical values for $\mathcal{Y} \sim 100$ GPa and $\mathcal{P} \sim 100$ MPa, we see that $\varepsilon \sim 0.1\%$. Such a small strain can be provided using conventional piezo crystals. For model A, ε up to 0.11% has already been realized in experiments, and in principle, ε up to 0.6% can be achieved[30,31]. For model B, it is more suitable to provide compressive stress along the z direction, and there is no limitation on the maximum ε because the compressive stress is not limited by the gluing technique. We assume $|\varepsilon| < 0.3\%$ the most probable regime that can be accessed in experiments. Since the lattice deformation is very small, the uniaxial stress has negligible effects on the superconductor transition temperature as well as the s-wave pairing symmetry[34,35], two properties that are crucial for the generation of Majorana fermions.

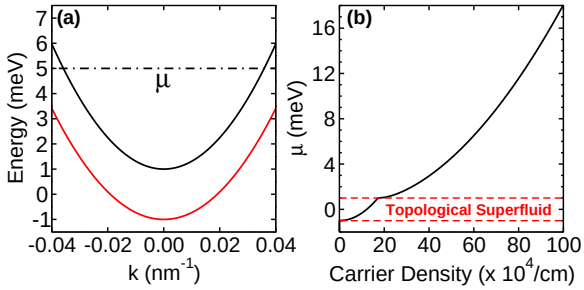

FIG. 2: (Color online) (a) Band structure of InSb nanowires. The solid horizontal dash-dotted line represents the possible pinned chemical potential when placed in proximity to the superconductor. (b) The chemical potential as a function of carrier density. $\alpha \sim 0.2$ eV·Å, $m = 0.013m_0$, $\Delta_0 = 0.5$ meV, $V_z = 1.0$ meV. Parameters are from Ref. 36.

The effective Hamiltonian for n-type nanowire under uniaxial stress reads as[38,39],

$$H = [\frac{k^2}{2m} + \alpha(\mathbf{p} \times \sigma)_z + V_z\sigma_z + a_c\mathrm{Tr}(\varepsilon)] - \mu_F. \qquad (2)$$

where a_c denotes the deformation potential of the conduction band, α is the spin-orbit coupling strength, and V_z is the external Zeeman field induced by the magnetic field. μ_F is the true chemical potential of the semiconductor that is pinned to the Fermi surface of the superconductor. The uniaxial stress does not change the band structure, but shifts the effective chemical potential to $\mu = \mu_F - a_c\mathrm{Tr}(\varepsilon)$, through which the topological region $V_z^2 > \Delta^2 + \mu^2$[15,16] may be achieved. In Fig. 2a, we plot the typical band structure of free electrons in nanowires in a single transverse confinement band and in Fig. 2b we plot the corresponding chemical potential as a function of carrier density. The topological superconductivity with MFs can be achieved when the chemical potential falls in the small window in Fig. 2b, in which case the system cuts only one Fermi surface. The small window in the parameter space greatly limits the flexibility for the experimental observation of MFs. For InSb, $a_c \sim -6.94$ eV, and $|\varepsilon| < 0.3\%$, we estimate $a_c\mathrm{Tr}(\varepsilon) \sim \pm 21$ meV, the same magnitude as the energy difference between the chemical potential of the nanowire and the conduction band minima in the Delft experiment[24]. We see from Fig. 2b that such a huge change of the effective chemical potential can change the carrier density by about 1 - 2 orders of magnitude. Thus, for a wide range of carrier density, the nanowire can always be tuned to the topological regime in the experiment.

The Hamiltonian for p-type nanowires (assuming the sizes along the y and z directions are L_y and L_z, respectively) under uniaxial stress reads as[37],

$$H = H_{\mathrm{KL}} + H_{\mathrm{BP}} - \mu_F, \qquad (3)$$

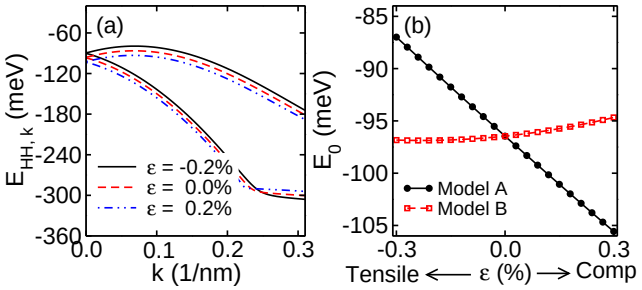

FIG. 3: (Color online). (a) Typical band dispersions of the heavy hole bands for different values of strain ε in model A. (b) Energy of heavy hole bands at $k = 0$ as a function of strain ε for models A and B. Other parameters are $\gamma_1 = 34.8$, $\gamma_2 = 15.5$, $\alpha = 2.0$ eV·Å, $V_z = 1.5$ meV, $L_z = 14$ nm, and $L_y = 10$ nm, $\mu = 0$. Parameters are from Ref. 36.

where $H_{\rm KL} = \frac{(2\gamma_1+5\gamma_2)}{4}\nabla^2 - \gamma_2(\nabla\cdot\mathbf{J})^2 - i\alpha(\mathbf{J}\times\nabla)_z + V_z J_z$ is the Kohn-Luttinger Hamiltonian, $\mathbf{J}$ is the total angular momentum operator for the spin-3/2 holes and γ_1 and γ_2 are Luttinger parameters. The second term describes the Bir-Pikus model[38–41]

$$H_{\rm BP} = \begin{pmatrix} P_\varepsilon + Q_\varepsilon & 0 & R_\varepsilon & 0 \\ 0 & P_\varepsilon - Q_\varepsilon & 0 & R_\varepsilon \\ R_\varepsilon^* & 0 & P_\varepsilon - Q_\varepsilon & 0 \\ 0 & R_\varepsilon^* & 0 & P_\varepsilon + Q_\varepsilon \end{pmatrix}, \quad (4)$$

where $P_\varepsilon = -a_v {\rm Tr}(\varepsilon)$, $Q_\varepsilon = -\frac{b}{2}(\varepsilon_{xx} + \varepsilon_{yy} - 2\varepsilon_{zz})$, $R_\varepsilon = \frac{\sqrt{3}}{2} b(\varepsilon_{xx} - \varepsilon_{yy})$, with a_v and b the deformation potentials of the valence bands. Notice that P_ε, Q_ε and R_ε have totally different roles to the band structures of holes in nanowires. P_ε shifts the global band structure, while Q_ε increases or decreases the splitting between the heavy hole (HH) and light hole (LH) bands. The nonzero R_ε may greatly enhance or suppress the coupling between HH and LH, thus modifying the effective pairing strength. In contrast to the case of electrons, the two models A and B yield totally different results.

The modification of the band structure of p-type nanowires due to uniaxial stress is shown in Fig. 3a for different values of ε. Here we only plot the two HH bands because the LH bands are separated by a large energy gap (~ 100 meV) induced by the confinement. At $k = 0$, two HH bands are split by a small Zeeman field V_Z. When the chemical potential lies in the Zeeman gap, the system has only a single Fermi surface, yielding topological superconductivity and the associated MFs under suitable conditions. We see from Fig. 3 that by tuning the uniaxial stress, we can shift the bands of the semiconductor up or down so that the Fermi level of the superconductor can lie in the Zeeman gap, yielding topological superconductivity. In Fig. 3b, we plot E_0, the energy of the HH bands at $k = 0$, against ε. Within the experimentally accessible regime, E_0 can be tuned by ± 3 meV for model B and ± 10 meV for model A.

To obtain concrete parameter regions of the MFs, the superconducting order parameter need be taken into account. Because the uniaxial stress only shifts the effective chemical potential for the n-type of semiconductor, we consider only p-type nanowires. In the nanowire heterostructures, the superconducting order parameter can be induced to the nanowire through proximity effect[42,43], yielding $H_{\rm sc} = \sum_{m=\frac{1}{2},\frac{3}{2}} \int d\mathbf{r} \Delta_m \psi_m^\dagger \psi_{-m}^\dagger$. The corresponding BdG Hamiltonian can be written as[19]

$$H_{\rm BdG} = \begin{pmatrix} H_{\rm 1D} & \Delta_4 \\ \Delta_4^* & -\gamma^\dagger H_{\rm 1D}^* \gamma \end{pmatrix} \quad (5)$$

in the Nambu spinor basis $\Psi = (\psi, \gamma\psi^\dagger)^T$. Here $H_{\rm 1D} = \int dydz \psi_y^* \psi_z^z H \psi_z \psi_y$, $\gamma = i(I \otimes \sigma_x)\tau_y$, σ_x, I and τ_y are Pauli operators, and $\Delta_4 = {\rm diag}(\Delta_{\frac{3}{2}}, \Delta_{\frac{1}{2}}, \Delta_{\frac{1}{2}}, \Delta_{\frac{3}{2}})$.

The topological parameter regime for MFs can be obtained by the topological index[44,45]

$$\mathcal{M} = {\rm sign}({\rm Pf}(\Gamma(0)) \cdot {\rm Pf}(\Gamma(\frac{\pi}{a}))) \quad (6)$$

where Pf(Γ) refers to the Pfaffian of the matrix $\Gamma = -iH_{\rm BdG}(k)(\tau_y \otimes \gamma)$, a is the lattice constant. $\mathcal{M} = +1$ (-1) corresponds to the topologically trivial (nontrivial) superconducting states without (with) MFs. Note that for sufficient large k all the eigenvalues of Γ are dominated by the k^2 terms, yielding ${\rm sign}({\rm Pf}(\Gamma(\frac{\pi}{a}))) = 1$. The Pfaffian at $k = 0$ can be derived analytically, yielding $\mathcal{M} = {\rm sgn}\mathcal{F}$, with $\mathcal{F} = f_0 - f_1 V_z^2 + \frac{9}{16} V_z^4$, $f_0 = (\bar{\mu}^2 + \Delta_{\frac{3}{2}}\Delta_{\frac{1}{2}} - \beta_1^2 - \beta_2^2)^2 + ((\Delta_{\frac{3}{2}} - \Delta_{\frac{1}{2}})\bar{\mu} + \beta_1(\Delta_{\frac{3}{2}} + \Delta_{\frac{1}{2}}))^2$, $f_1 = (10\bar{\mu}^2 + 10\beta_1^2 + 16\beta_1\bar{\mu} + 9\Delta_{\frac{1}{2}}^2 + \Delta_{\frac{3}{2}}^2 - 6\beta_2^2)/4$, $\beta_1 = \pi^2\gamma_2(L_z^{-2} - L_y^{-2}/2) + Q_\varepsilon$, $\beta_2 = \sqrt{3}\pi^2\gamma_2 L_y^{-2}/2 + R_\varepsilon$, and $\bar{\mu} = \mu + \gamma_1\pi^2(L_y^{-2} + L_z^{-2}/2)$[46]. The boundary for topological phase transition is determined by $\mathcal{F} = 0$. Generally, the magnitudes of $\Delta_{\frac{3}{2}}$ and $\Delta_{\frac{1}{2}}$ are not essential for the topological quantum phase transition (but the relative sign is important)[19]. Henceforth we only consider two different possible cases (I) $\Delta_{\frac{3}{2}} = \Delta_{\frac{1}{2}} = \Delta$ and (II) $\Delta_{\frac{3}{2}} = -\Delta_{\frac{1}{2}} = \Delta$. For other values of $\Delta_{\frac{3}{2}}$ and $\Delta_{\frac{1}{2}}$, the results are similar.

In Fig. 4a and 4b, we plot the boundary between the topological and non-topological superconducting states. In these figures, we assume that without uniaxial stress the chemical potential lies in a regime which requires a large Zeeman field for realizing the topological superconducting state. By applying the uniaxial stress the required critical Zeeman field can be significantly reduced. In case (I) in Fig. 4a, the critical Zeeman field can even approaches zero for model A. We have also verified that for a wide range of parameters (μ, L_z, L_y $\cdots$) similar features can always be found. For case (II) in Fig. 4b the required Zeeman field can be reduced to around 1 meV ($B_z = 0.3$ T for $g_h^* \sim 50$). Generally for case (II), the minimum required $V_z^c \simeq p\Delta$, where $p = 2\sqrt{1 + \beta_1^2/\beta_2^2}/(2 + \sqrt{1 + \beta_1^2/\beta_2^2}) \in [2/3, 2)$. We see that there are also a wide range of parameters that enable us to achieve the minimum required Zeeman field at $p = 2/3$ via uniaxial stress. To further verify that

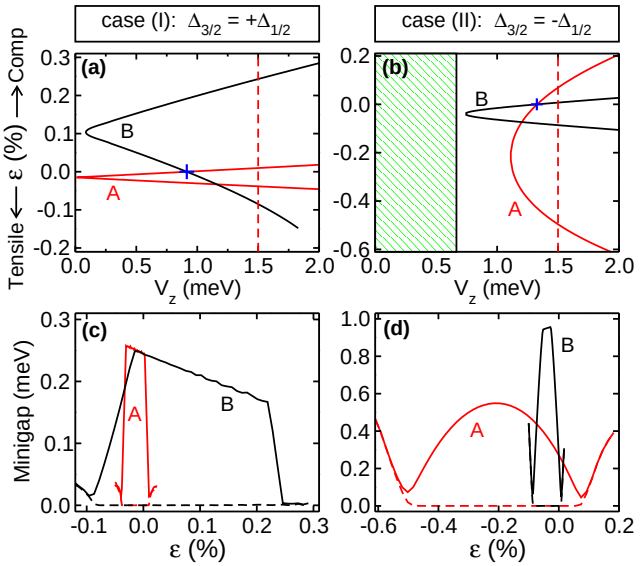

FIG. 4: (Color online). The parameter regimes for the existence of Majorana fermions. (a), (b) show the results for case (I) and case (II), respectively, see text for details. The plus sign (+) corresponds to V_z without uniaxial stress. For case (I) we use $L_y \simeq 10.0$ nm, $L_z \simeq 14.0$ nm, for case (II) we use $L_y \simeq 14.2$ nm, $L_z \simeq 9.7$ nm. The chemical potential in all the figures are pinned at $\mu = -96.0$ meV. In (b) the shaded regime corresponds to the lower bound of $V_z/\Delta = 2/3$. The corresponding mini-gap and lowest non-negative energy level obtained by numerically solving the BdG Eq. (5) are presented in (c) and (d), respectively, for $V_z = 1.5$ meV. The other parameters are the same as Fig. 3.

the right regime of each curve in Fig. 4a and 4b are indeed the topological superconducting regime we plot the mini-gap (solid line) and the lowest non-negative energy level (dashed line) as a function of uniaxial stress ε in Figs. 4c and 4d, respectively. In the topological superconducting state, the zero energy MFs indeed exist with large minigaps around several Kelvin. We have also confirmed that the corresponding wavefunctions of MFs are well localized at the two ends of the nanowire.

The difference between the two types of uniaxial stress in models A and B can be understood by projecting the Hamiltonian to the lowest two HH bands[37–41,46,47], which yields the effective pairing at $k \to 0$,

$$\Delta_{\text{eff}} = (\Delta_{\frac{3}{2}} - \kappa\Delta_{\frac{1}{2}})/(\kappa + 1) \qquad (7)$$

where $\kappa = (\sqrt{(\beta_1/\beta_2)^2 + 1} - \beta_1/\beta_2)^2 \in (0, \infty)$. When $\varepsilon = 0$, κ only depends on the size of the nanowire, thus cannot be tuned. However, when the uniaxial stress is applied, κ can be tuned in a considerably wide range. For model A, the off-diagonal term $R_\varepsilon \neq 0$, thus β_2 can approach zero with a properly chosen strain ε. For the parameters used in Fig. 4 we find that the effective pairing increases (decreases) monotonically as a function of ε for model A (B), thus for model B, we observe significant enhancement of the mini-gap ($\sim 30\%$) in Fig. 4d. The maximum increase of the mini-gap can be obtained by optimizing different physical parameters.

Finally, several remarks are in order. First, the same idea discussed above for a single band model can be straightforwardly extended to the multiband case. Using the diameter of nanowire from Ref.[24], we estimate the band spacing for electron (hole) is ~ 6 (~ 3) meV, with ~ 4 bands occupied. Thus we expect that the stress can tune the effective chemical potential of both electrons and holes to the topological regime even though the initial value corresponds to an even number of Fermi surfaces. Second, our proposal here can also be used to engineer MFs in the vortex core of semiconductor quantum wells. For electrons the tuning of the band structures is exactly the same as in Eq. 2. For holes there are some qualitative difference from Fig. 3 since the confinement along the y direction is relaxed. As a consequence, $\beta_2 = 0$ when $\varepsilon = 0$, thus R_ε play a more significant role in the determination of the minigap of MFs. Third, we have also checked the validity of our proposal for InAs nanowires, and similar features have been found. However, for InAs, we note that[36] $a_c \sim -5.17$ and $b \sim -1.00$, which are smaller than their counterparts in InSb, thus a slightly larger stress is required.

To conclude, due to the proximity effect between nanowires and a bulk superconductor, the chemical potential of the nanowire is generally pinned by the Fermi surface of the superconductor. Consequently, tuning the chemical potential of nanowires via electrical gates to bring it in the topological regime is inefficient in this setup. We show that this crucial obstacle can be overcome using experimentally accessible uniaxial stress which modifies the band structure slightly, leading, remarkably, to a transition from non-topological to topological states with MFs. The newly added elements for generating uniaxial stress can be effectively integrated into the design of semiconductor devices using modern nanotechnology. Therefore our scheme can be used for the realization of topological Majorana fermion excitations in semiconductors and the implementation of topological quantum computation.

Acknowledgement: We thanks valuable discussions with K. D. Jons and J. D. Plumhof about the experimental implementation of unaxial stress and P. Kouwenhoven about the possible pinning of chemical potential in their experiments. This work is supported by DARPA-MTO (FA9550-10-1-0497), DARPA-YFA (N66001-10-1-4025), and NSF-PHY (1104546 and 1104527).

* Corresponding Author; Email: chuanwei.zhang@utdallas.edu

[1] E. Majorana, Nuovo Cimento **14**, 171 (1937).

[2] F. Wilczek, Nature Physics **5**, 614 (2009).
[3] M. Frantz, Physics **3**, 24 (2010).
[4] A. Kitaev, Ann. Phys. (N.Y.) **303**, 2 (2003).
[5] C. Nayak, S. H. Simon, A. Stern, M. Freedman and S. Das Sarma, Rev. Mod. Phys. **80**, 1083 (2008).
[6] N. Read and D. Green, Phys. Rev. B **61**, 10267 (2000).
[7] S. Das. Sarma, M. Freedman and C. Nayak, Phys. Rev. Lett. **94**, 166802 (2005).
[8] P. Bonderson, A. Kitaev and K. Shtengel, Phys. Rev. Lett. **96**, 016803 (2006).
[9] A. Stern and B. I. Halperin, Phys. Rev. Lett. **96**, 016802 (2006).
[10] S. Das Sarma, C. Nayak, S. Tewari, Phys. Rev. B **73**, 220502 (R) (2006).
[11] J. D. Sau, Roman M. Lutchyn, Sumanta Tewari and S. Das Sarma, Phys. Rev. Lett. **104**, 040502 (2010).
[12] J. Alicea, Phys. Rev. B **81**, 125318 (2010).
[13] J. Sau, S. Tewari, R. M. Lutchyn, T. D. Stanescu and S. Das Sarma, Phys. Rev. B **82**, 214509 (2010).
[14] A. C. Potter and Patrick A. Lee, Phys. Rev. Lett. **105**, 227003 (2010).
[15] Y. Oreg, G. Refael and F. von Oppen, Phys. Rev. Lett. **105**, 177002 (2010).
[16] R. M. Lutchyn, J. D. Sau, S. Das Sarma, Phys. Rev. Lett. **105**, 077001 (2010).
[17] L. Mao, C. Zhang, Phys. Rev. B **82**, 174506 (2010).
[18] L. Mao, J. Shi, Q. Niu, C. Zhang, Phys. Rev. Lett. **106**, 157003 (2011).
[19] L. Mao, M. Gong, E. Dumitrescu, S. Tewari and C. Zhang, Phys. Rev. Lett. **108**, 177001 (2012).
[20] C. W. J. Beenakker, arXiv:1112.1950.
[21] C. Zhang, S. Tewari, R. M. Lutchyn and S. Das Sarma, Phys. Rev. Lett. **101**, 160401 (2008).
[22] S. Sasaki, M. Kriener, K. Segawa, K. Yada, Y. Tanaka, M. Sato, and Y. Ando, Phys. Rev. Lett. **107**, 217001 (2011).
[23] J. R. Williams, A. J. Bestwick, P. Gallagher, Seung Sae Hong, Y. Cui, Andrew S. Bleich, J. G. Analytis, I. R. Fisher, D. Goldhaber-Gordon, Phys. Rev. Lett. **109**, 056803 (2012).
[24] V. Mourik, K. Zuo, S. M. Frolov, S. R. Plissard, E. P. A. M. Bakkers and L. P. Kouwenhoven, Science, 336, 1003 (2012).
[25] M. T. Deng, C. L. Yu, G. Y. Huang, M. Larsson, P. Caroff, H. Q. Xu, Nano Lett. **12**, 6414 (2012).
[26] L. P. Rokhinson, X. Liu, J. K. Furdyna, Nature Physics **8**, 795 (2012).
[27] A. Das, Y. Ronen, Y. Most, Y. Oreg, M. Heiblum, H. Shtrikman, Nature Physics **8**, 887 (2012).
[28] J. D. Sau, C. H. Lin, H.-Y. Hui and S. Das Sarma, Phys. Rev. Lett. **108**, 067001 (2012).
[29] M. Shayegan, K. Karrai, Y. P. Shkolnikov, K. Vakili, E. P. De Poortere, and S. Manus, Appl. Phys. Lett **83**, 5235 (2003).
[30] C. Thiele, K. Dörr, O. Bilani, J. Rödel and L. Schultz, Phys. Rev. B **75**, 054408 (2007).
[31] J. D. Plumhof, V. Krapek, F. Ding, K. D. Jons, R. Hafenbrak, P. Klenovsky, A. Herklotz, K. Dorr, P. Michler, A. Rastelli and O. G. Schmidt, Phys. Rev. B **83**, 121302(R), (2011).
[32] K. D. Jons, R. Hafenbrak, R. Singh, F. Ding, J. D. Plumhof, A. Rastelli, O. G. Schmidt, G. Bester, and P. Michler, Phys. Rev. Lett. **107**, 217402 (2011).
[33] Stefan Seidl, Martin Kroner, Alexander Hogele, Khaled Karrai, Richard J. Warburton, Antonio Badolato, and Pierre M. Petroff, Appl. Phys. Lett. **88**, 203113 (2006).
[34] H. D. Yang, J.-Y. Lin, H. H. Li, F. H. Hsu, C. J. Liu, S.-C. Li, R.-C. Yu, and C.-Q. Jin, Phys. Rev. Lett. **87**, 167003 (2001).
[35] X. J. Chen, H. Zhang and H. U. Habermeier, Phys. Rev. B. **65**, 144514 (2002).
[36] I. Vurgaftmana, J. R. Meyer and L. R. Ram-Mohan, J. Appl. Phys. **89**, 5815 (2001).
[37] B. A. Bernevig, and S.-C Zhang, Phys. Rev. Lett. **95**, 016801 (2005).
[38] S.-H. Wei and A. Zunger, Phys. Rev. B **49**, 14337 (1994).
[39] M. Gong, K. Duan, C.-F. Li, R. Magri, G. A. Narvaez, and L. He, Phys. Rev. B **77**, 045326 (2008).
[40] L. He, G. Bester, and A. Zunger, Phys. Rev. B **70**, 235316 (2004).
[41] C. Pryor, J. Kim, L.-W. Wang, A. J.Williamson, and A. Zunger, J. Appl. Phys. **83**, 2548 (1998).
[42] Y.-J. Doh, J. A. van Dam, A. L. Roest, E. P. A. M. Bakkers, L. P. Kouwenhoven and S. De Franceschi, Science **309**, 272 (2005).
[43] J. Xiang, A. Vidan, M. Tinkham, R. M. Westervelt and C. M. Lieber, Nature Nanotechnology **1**, 208 (2006).
[44] A. Yu. Kitaev, Physics-Uspekhi (supplement) **44**, 131 (2001).
[45] P. Ghosh, J. D. Sau, S. Tewari, S. Das Sarma, Phys. Rev. B, **82**, 184525 (2010).
[46] See the supplemental material for details.
[47] R. Winkler, "Spin-orbit coupling effects in two-dimensional electron and hole systems", Springer Tracts in Modern Physics, Vol. 191 (Springer-Verlag, Berlin, 2003).